Received: 18 February 2023 | Revised: 29 March 2023 | Accepted: 10 April 2023

DOI: 10.1002/agt2.344

Aggregate WILEY Open Access

RESEARCH ARTICLE

Ultralong excimer phosphorescence by the self-assembly and confinement of terpyridine derivatives in polymeric matrices

Guangqiang Yin[1,2] | **Wei Lu**[1,2] | **Jianxiang Huang**[3] | **Rui Li**[1,2] | **Depeng Liu**[1,2] | **Longqiang Li**[1,2] | **Ruhong Zhou**[3] | **Guifei Huo**[4] | **Tao Chen**[1,2]

[1]Key Laboratory of Marine Materials and Related Technologies, Zhejiang Key Laboratory of Marine Materials and Protective Technologies, Ningbo Institute of Materials Technology and Engineering, Chinese Academy of Sciences, Ningbo, China

[2]School of Chemical Sciences, University of Chinese Academy of Sciences, Beijing, China

[3]Institute of Quantitative Biology, College of Life Sciences, Zhejiang University, Hangzhou, China

[4]Department of Chemistry, National University of Singapore, Singapore, Singapore

Correspondence
Wei Lu and Tao Chen, Key Laboratory of Marine Materials and Related Technologies, Zhejiang Key Laboratory of Marine Materials and Protective Technologies, Ningbo Institute of Materials Technology and Engineering, Chinese Academy of Sciences, Ningbo 315201, China.
Email: luwei@nimte.ac.cn; tao.chen@nimte.ac.cn

Guifei Huo, Department of Chemistry, National University of Singapore, 117543, Singapore.
Email: chmguif@nus.edu.sg

Funding information
National Key Research and Development Program of China, Grant/Award Numbers: 2022YFB3204301, 2021YFA1201201; National Natural Science Foundation of China, Grant/Award Numbers: 22205249, U1967217; China Postdoctoral Science Foundation, Grant/Award Numbers: 2021TQ0341, 2022M723252; Zhejiang Provincial Natural Science Foundation of China, Grant/Award Number: LQ23B040002; Natural Science Foundation of Ningbo, Grant/Award Number: 2021J203; Foundation of the Director of NIMTE, Grant/Award Number: 2021SZKY0305

Abstract

Ultralong organic room temperature phosphorescence (RTP) is attracting increasing attention due to its fascinating optical phenomena and wide applications. Among various RTP, excimer phosphorescence is of fundamental significance, but it remains a considerable challenge to achieve flexible, multicolor and large-area excimer RTP materials, which should greatly advance the understanding and development of organic light-emitting devices. Herein, we present ultralong excimer RTP films by the self-assembly and confinement of terpyridine (Tpy) derivatives in polymeric matrices. Strikingly, the self-assembly of Tpy derivatives induces the formation of excimer complexes, thus immensely minimizing singlet-triplet splitting energy (ΔE_{ST}) to promote the intersystem crossing process. Furthermore, the confinement by multiple hydrogen bonding interactions as well as the compact aggregation of phosphors jointly suppresses the nonradiative transitions, leading to long-lived excimer RTP (τ = 543.9 ms, 19,000-fold improvements over the powder). On account of the outstanding afterglow performance and color-tunability of RTP materials, flexible and large-area films were fabricated for intelligent display, anticounterfeiting, and time-resolved information encryption.

KEYWORDS
aggregation, excimer, information encryption, room temperature phosphorescence, terpyridine

1 | INTRODUCTION

Purely organic materials with ultralong afterglow emission have been widely applied in bioimaging,[1–4] organic light-emitting diodes,[5] sensors,[6–10] data encryption,[11–13] and so on. Unlike inorganic phosphors containing rare, toxic, and expensive elements,[14] organic room temperature phosphorescence (RTP) materials possess inherent merits of outstanding performance with color-tunable properties, eco-friendliness, and mild preparation conditions.[15–20] To date, several effective strategies have been successfully developed to access ultralong RTP mainly based on the promotion of intersystem crossing (ISC) and the suppression of the nonradiative decay of triplet excitons, such as crystal engineering,[21–23] H-aggregation,[24,25] polymerization,[26–29] host–guest systems,[30–33] heavy-atom designs,[34,35] formation of aggregates,[1,36–39] construction of frameworks,[40,41] and doping in polymeric matrices.[42–44] These effective preparation methods have significantly advanced the development of ultralong organic RTP materials and provided them with more opportunities for practical applications.[45]

Among a wide variety of RTP systems, the study of excimer phosphorescence is of fundamental significance and should greatly advance the understanding of energy/charge transfer and intermolecular interactions in plenty of organic optoelectronic devices, thus promoting the design and development of related devices.[46–51] Excimer, namely,

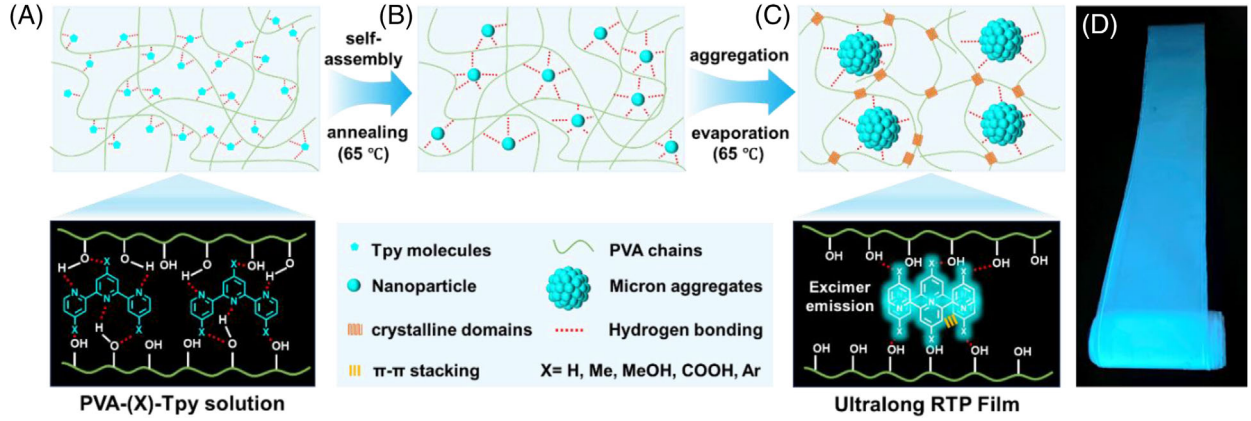

SCHEME 1 Illustration of the preparation of ultralong room temperature phosphorescence (RTP) film. (A) The precursor solution of poly(vinyl alcohol) (PVA) and terpyridine (Tpy) derivatives at 96°C. (B) The self-assembly of Tpy derivatives into nanoparticles via thermal annealing at 65°C. (C) The aggregation of Tpy nanoparticles into micron aggregates and their strong confinements in the PVA matrix during drying process to form ultralong RTP film. (D) A roll of flexible and large-area PVA-Tpy film under 254-nm ultraviolet (UV) light.

excited-state homodimer, often has a significant impact on the photophysical properties of chromophores in organic light-emitting devices.[52–57] In sharp contrast to extensive investigations of the steady-state fluorescence of singlet-state excimer, the phosphorescence from triplet excimer is far from well understood attributed to the lack of theoretical and experimental authentication. As one of the host-guest systems, the pioneering exciplex (heterodimeric species)-based RTP by Kabe and Adachi was realized by the recombination of charge-separated states.[58,59] In such a well-known RTP system, both electron-donating and electron-accepting molecules should be carefully selected to form exciplex with a long-lived charge-separated state.[60] Differently, excimer phosphorescence occurs owing to a tight association of homodimeric species, particularly in the cases of polyaromatic hydrocarbons, such as naphthalene and phenanthrene.[61–64] The challenge of achieving excimer phosphorescence is not only attributed to the low spin-orbit coupling (SOC) of aromatic compounds but also due to difficulty in the stabilization of short-lived excimer to harvest triplet excitons.[65,66] In recent years, triplet excimer emission has been successfully realized in the crystalline state of planar luminophores, demonstrating that the strong π-π interactions among phosphors play an important role in excimer phosphorescence.[67–70] However, the realization of excimer phosphorescence in the polymeric matrix to achieve flexible, multicolor and large-area RTP films remains a formidable challenge, because there exists a great difficulty in the controllable self-assembly and population of triplet excimer in such a complicated system.

In this context, we rationally selected a series of 2,2′:6′,2′′-terpyridine (Tpy) derivatives as phosphors and integrated them with semicrystalline poly(vinyl alcohol) (PVA) to render ultralong excimer RTP materials (Scheme. 1). The heterocyclic polynuclear Tpy fluorophore containing N heteroatoms favor an n−π* transition for boosting the ISC process, which is beneficial to populating triplet excitons under ambient conditions.[71–74] In addition, the geometric confinement effect of the rigid PVA matrix by the multiple hydrogen bonding between Tpy phosphors and PVA chains can greatly enhance SOC and effectively inhibit nonradiative decay rates.[16] More importantly, the coassembly of Tpy molecules to form excimer complexes immensely minimizes the energy gap (ΔE_{ST}) between singlet and triplet states, which is conducive to the ISC process. As such, the resultant ultralong RTP materials exhibited excellent afterglow performance with flexible, transparent and color-tunable properties, and could be readily processed into films, fibers, and coatings in large-area for afterglow display, anticounterfeiting and time-resolved information encryption. This study not only demonstrates an effective strategy to fabricate flexible, multicolor, and large-area excimer RTP but also broadens the scope of afterglow materials for advanced applications.

2 | RESULTS AND DISCUSSION

2.1 | The preparation and optical characterization of ultralong RTP films

The ultralong RTP film was facilely fabricated by a simple drop-casting and thermal annealing method. A clear and homogeneous precursor solution was obtained after stirring the mixed aqueous solution of hydrophobic Tpy and PVA at 96°C for 45 min (Scheme 1A, Figure S2). The obtained precursor solution was transferred to thermal annealing immediately at 65°C for 15 min (Scheme 1B). The free-standing PVA-Tpy film was fabricated after drying at 65°C for 1 h (Scheme 1C, see SI for experimental details). Unexpectedly, the steady-state (prompt) fluorescence spectrum of PVA-Tpy film reveals dual-band emission at around 350 nm from local emission (LE, "monomer" emission), and a prominent emission at 465 nm ascribed to the excimer emission (Figure 1A). Notably, the time-resolved (delayed) spectrum displays a typical long persistent luminescence character in that a dominating emission at 485 nm with intense cyan afterglow. The average lifetime of the phosphorescence at 485 nm was measured as 543.9 ms under ambient conditions (Figure 1B), revealing a long-lived feature. It was also found that the process of thermal annealing has a marked impact on the afterglow properties and excimer emission (Figure S54). Delayed emission−excitation mapping of PVA-Tpy film manifests that the emission band is independent of excitation wavelength and the optimal excitation wavelength is around 240 nm (Figure 1C). The phosphorescence intensity and lifetime were progressively decreased upon increasing

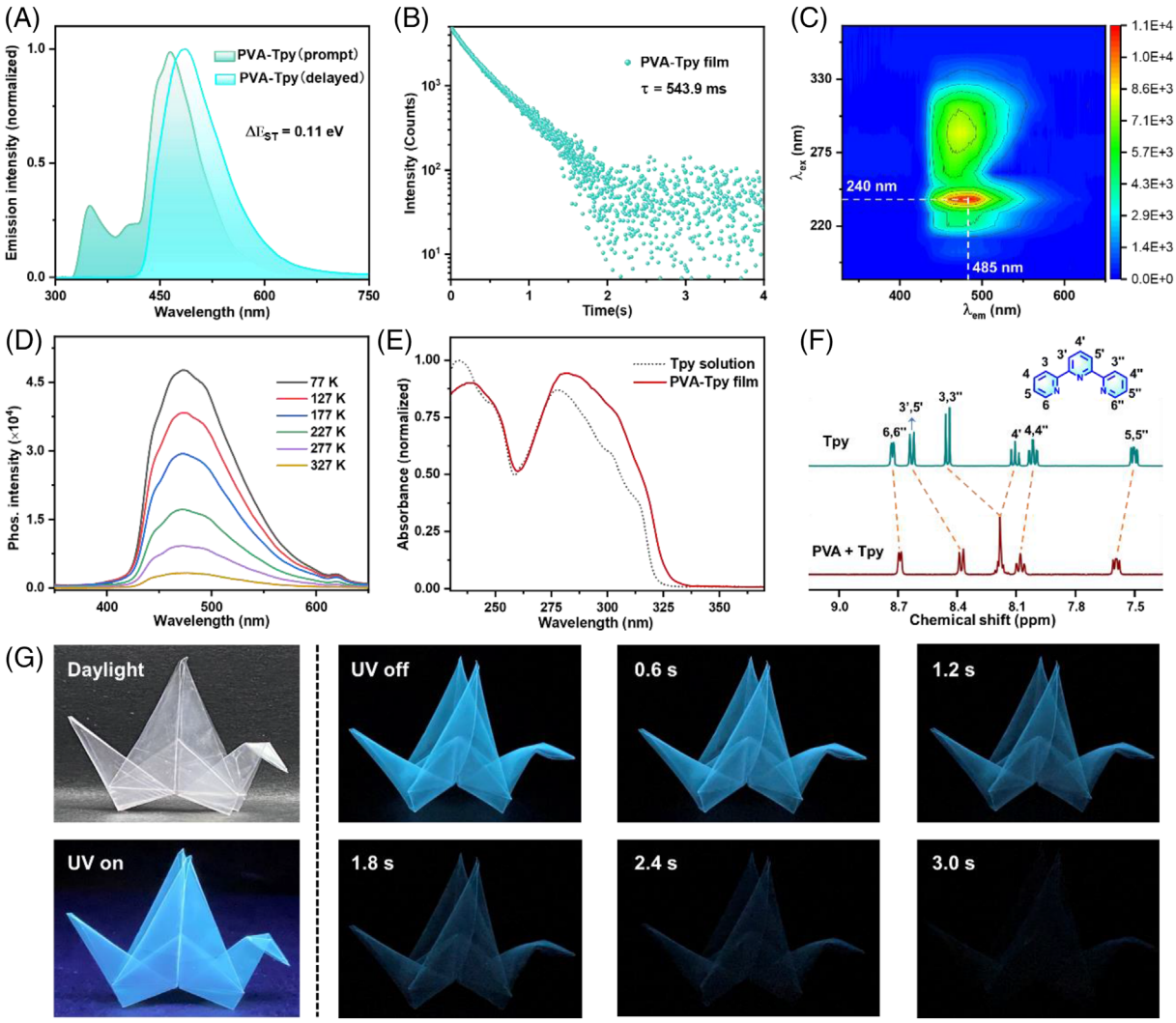

FIGURE 1 The photophysical characterization of PVA-Tpy film. (A) Prompt and delayed emission spectra of PVA-Tpy film, λ_{ex} = 240 nm. (B) Time-resolved emission-decay profile of PVA-Tpy film at 485 nm. (C) Delayed emission−excitation mapping of PVA-Tpy film. (D) Temperature-dependent delayed emission spectra of PVA-Tpy film from 77 to 327 K, λ_{ex} = 240 nm, delayed time: 0.05 ms. (E) Ultraviolet-visible (UV-vis) absorption spectra of PVA-Tpy (1.0 wt%) film and Tpy solution (5×10^{-6} M). (F) ^{1}H nuclear magnetic resonance (NMR) spectra (aromatic region) of Tpy in d_6-Dimethyl sulfoxide (DMSO) and PVA+Tpy (1.0 wt%) in D_2O at 298 K. (G) Photographs of the origami crane show long-lived delayed emission under 254-nm UV excitation and at different time intervals after erasing UV irradiation.

the temperature from 77 to 327 K (Figure 1D and Figure S49), presumably owing to the thermal sensitivity of the aggregates and increased molecular motions of both Tpy phosphors and PVA chains, which excluded the assignment of delayed emission to thermally activated delayed fluorescence. Moreover, complicated 3D objects such as origami cranes could be fabricated based on the flexibility and tailorability of PVA-Tpy film (Figure 1G). It exhibits long-lived phosphorescence with a visible afterglow duration of 2.4 s (Video S1). The afterglow emission hardly changed in color and only slowly faded in cyan upon the removal of the ultraviolet source. Longer afterglow was visible to the naked eye for about 5 s at 77 K (Video S2).

2.2 | Experimental authentication of the excimer phosphorescence

The photophysical property of the film was further studied by ultraviolet-visible (UV-vis) absorption spectroscopy. The broadening of the absorption bands along with small red-shifts in maxima peaks indicated the preassociation of Tpy molecules in the PVA matrix (Figure 1E).[75–76] Moreover, the excitation spectra provided compelling evidence for the formation of excimer, exhibiting red-shifting and broadening feature of PVA-Tpy film compared with Tpy solution (Figure S56). The crystallinity of PVA matrix was characterized by powder X-ray diffraction (Figure S3). The concentration-dependent fluorescence proved the formation of excimer in a highly concentrated solution (Figure S4).

Considering the concentration-dependence of molecular interactions, we decided to investigate the impact of the doping concentration of Tpy phosphor on the optical performance of RTP films. As shown in Figure 2A, despite gradually diminution, the LE at around 350 nm remained even at high concentrations of 1.8 wt%. Differently, the excimer emission was increased at first due to the reduction of intermolecular distance and the increase of the probability of collisional interaction of excited and ground state monomers, and then descended obviously when increasing doping concentration of Tpy phosphor. The delayed emission revealed the same trend with steady-state excimer emission,

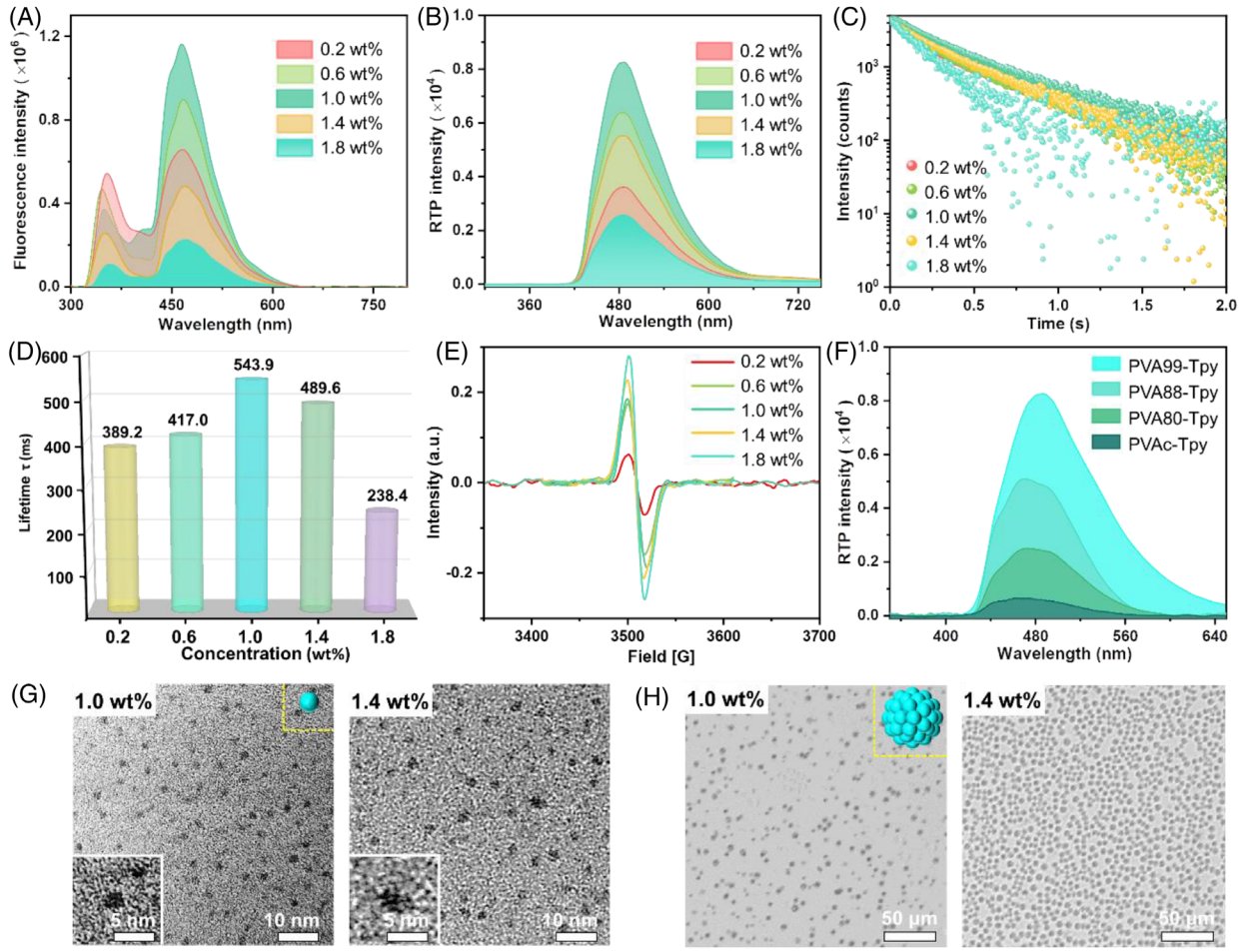

FIGURE 2 The experimental authentication of ultralong excimer room temperature phosphorescence (RTP). (A) Prompt fluorescence spectra, (B) delayed emission spectra, (C) time-resolved phosphorescence decay profiles (delayed time: 0.05 ms), (D) phosphorescence emission lifetimes, (E) electron paramagnetic resonance (EPR) spectra of poly(vinyl alcohol) (PVA)-terpyridine (Tpy) film with different doping concentrations (0.2–1.8 wt%). (F) Delayed emission spectra of PVA99-Tpy, PVA88-Tpy, PVA80-Tpy, PVAc-Tpy films, respectively (delayed time: 0.05 ms). (G) Transmission electron microscopy (TEM) images of annealed PVA-Tpy solution with doping concentrations of 1.0 and 1.4 wt%. (H) Optical microscopy (OM) images of PVA-Tpy films with doping concentrations of 1.0 and 1.4 wt%.

presenting the strongest emission at a concentration of 1.0 wt% (Figure 2B). It could be inferred that the ultralong RTP of the films should be closely corelative with the formation of excimer. The RTP lifetime of these films were measured as 389.2, 417.0, 543.9, 489.6, 238.4 ms, respectively (Figures 2C,D). These results suggested that the the optimal doping concentration was 1.0 wt%, demonstrating excessive content of Tpy molecules might significantly reduce the crystallinity of the PVA matrix. Further increase of doping concentration facilitates the formation of excimer but also reduces the RTP intensity and transparency of the material (Figure S58). Although electron paramagnetic resonance (EPR) spectra manifested that more triplet excitons were generated as doping concentration increased (Figure 2E), a plethora of Tpy molecules were inadequate to be effectively localized and confined in the polymeric matrix, resulting in triplet quenching.

In order to gain more insights into the mechanism of ultralong RTP, transmission electron microscopy, optical microscopy and scanning electron microscopy (SEM) were employed to study the self-assembly of Tpy phosphors in the polymeric matrix. After being dispersed into the PVA matrix, Tpy molecules were prone to form uniform nano-aggregates with an average diameter of 1–3 nm during thermal annealing (Figure 2G and Figures S5–S10), which contributed to the formation of excimer. Interestingly, these nanoparticles further merged into micron-scale aggregates after drying to form RTP films (Figure 2H and Figure S11). Although the microscopic morphologies of Tpy aggregates in these films are quite different, the optical properties and spectral profiles are similar, except for the ratio of LE to excimer emission is increased when increasing doping concentration (Figure S53). SEM images of these ultralong RTP films revealed smooth and uniform morphologies (Figure S12), demonstrating well distribution of Tpy aggregates in the PVA matrix. Besides, the aggregation behavior of Tpy molecules was further validated by nuclear magnetic resonance (NMR) including ^{1}H NMR and variable-temperature ^{1}H NMR (VT-^{1}H NMR). The characteristic resonance peaks of $H^{4'}$, $H^{4',4''}$, and $H^{5,5''}$ were shifted toward downfield slightly, while protons of $H^{3',5'}$, $H^{3,3''}$, and $H^{6,6''}$ were significantly shifted to upfield ($\Delta\delta$ = 0.25 ppm for $H^{3',5'}$), because of shielding effect from the molecular aggregation (Figure 1F and Figure S13). VT-^{1}H NMR displayed that all protons of Tpy were prominently moved to downfield as the temperature raised (Figure S14), possibly ascribed to the dissociation of Tpy aggregates. Furthermore, the offset face-to-face packing with a close distance of 0.37 nm of

Tpy molecules indicates there are strong π–π stacking interactions for driving the self-assembly and aggregation of Tpy molecules (Figure S51). The band broadening and significant redshift of the UV absorbance of PVA-Tpy film with increasing the doping concentration of Tpy also demonstrate the existence of intermolecular π-π stacking of Tpy molecules (Figure S52).[77] Evidently, these results substantiate that Tpy molecules are self-assembled into uniform aggregates driven by π–π stacking interactions, which facilitates the excimer emission owing to reduction of the intermolecular distance.

To figure out the effect of the strong confinement by hydrogen bonding on the RTP properties, attenuated total reflectance-Fourier transform infrared spectroscopy was first carried out. As compared to the pure PVA film, stretching vibrations of the hydroxy group (−OH) were blue-shifted from 3281 to 3260 cm^{-1} upon increasing doping concentration up to 1.8 wt% (Figure S15), which confirmed the formation of strong hydrogen bonding between PVA and Tpy molecules. Additionally, PVA with different alcoholysis degrees (99, 88, and 80%, denoted as PVA99, PVA88, and PVA80) and poly(vinyl acetate) (PVAc) were applied to verified the importance of hydrogen bonding interactions. As the alcoholysis degree of PVA decreased, the RTP performance was degraded apparently due to insufficient confinement of triplet exciton (Figure 2F and Figure S16). To further substantiate the conclusion that long-lived RTP originated from the hydrogen bonding, we also checked the afterglow performance of Tpy doped with different polymer matrices (Figure S17). It demonstrated that the RTP films exhibited excellent afterglow properties by introducing Tpy into those polymers could offer abundant hydrogen bonds. By contrast, with a lack of effective confinement from the rigid polymeric matrices, Tpy powder revealed poor RTP performance with a broad emission band (Figure S18). Only a faint afterglow with a duration of 0.3 s was observed (Figure S19), and its lifetime was measured as 28 μs (Figure S20). As such, it could be certainly deduced that the outstanding afterglow performance of PVA-Tpy film was closely correlated with hydrogen bonding between phosphors and PVA chains. By the means of being doped with PVA matrix, the lifetime was improved by more than 19,000-fold compared with that of the Tpy phosphor in the powder state. Overall, these results definitely proved that the ultralong RTP ascribed to the synergistic effect of the self-assembly and aggregation of Tpy molecules via π–π stacking interactions and the vibrational restriction by confinement from hydrogen bonding interactions.

2.3 | Theoretical simulations to verify the excimer phosphorescence

The aggregation of Tpy molecules and hydrogen bonding interactions in the PVA matrix was further elucidated by molecular dynamics simulations (Figure S21). Indeed, the Tpy molecules tend to clump togther through π–π stacking interactions, especially for the situation of high doping concentration (Figure S21a). The number of cofacial dimer, hydrogen bonds, and aggregation degree are all increased as the doping concentration raised (Figure S21b,d).

To better understand the observed long-lived afterglow emission from a purely organic system, we calculated the optoelectronic properties of Tpy monomer and dimer in singlet and triplet excited states using density functional theory with B3LYP functional[78] and the 6-31G(d,p) basis set[79] (Figure 3 and Figures S22–S24). The Tpy monomer and dimer display similar highest occupied molecular orbital (HOMO) energies, lowest unoccupied molecular orbital (LUMO) and spatial distribution (Figure 3A). Strikingly, both HOMO and LUMO are uniformly distributed over the perfectly cofacial dimer owing to intense π–π stacking, which is considered to play a critical role in the formation of triplet excimer.[68] As shown in Figure 3B, the lowest singlet (E_{S1} = 4.44 eV) and triplet (E_{T1} = 4.14 eV) excited states of Tpy monomer are quite close with a narrow energy gap (ΔE_{ST} = 0.30 eV), which promotes the singlet-triplet ISC process.[80] In addition, singlet-triplet splitting energy was further narrowed down to 0.14 eV for the dimer, indicating more favorable ISC to form a triplet excimer. The T_1 spin density of the Tpy dimer is mainly distributed on one molecule of the dimer complex and slightly on the other one (Figure 3C), which is indicative of a minor difference in RTP emission between the Tpy monomer and dimer. However, the phosphorescence peaks of monomer and excimer are close to their corresponding fluorescent emission as evidenced by pure LE and excimer emission in dilute and highly concentrated solutions, respectively (Figure S25). The delayed emission of dilute and highly concentrated Tpy solution undergo double-exponential and triple-exponential decays with lifetime of 2.65 μs and 9.82 μs, respectively (Figure S57). It was also found that the maxima of excimer phosphorescence and fluorescence of Tpy solution are almost overlap ascribed to low ΔE_{ST}. As such, the triplet excimer of PVA-Tpy film is probably not originated from direct ISC of excited dimer. Taken together, we proposed a rational mechanism that led to ultralong excimer RTP as depicted in Figure 3D. The ground-state Tpy monomers (S_0) were excited to singlet state (S_1) upon excitation and a portion of the excited monomers would revert to S_0 by radiative transition (LE). Meanwhile, partial singlet monomers underwent a spin-forbidden ISC process to the triplet state (T_1). Theoretically, monomer phosphorescence should be observed. However, the strong π–π stacking interactions in the compact aggregates greatly facilitates the energy transfer from triplet monomer to an adjacent molecule in the S_0, ultimately resulting in harvesting triplet excimer (T_1*).[70] In addition, the multiple hydrogen bonds immensely stabilized the Tpy aggregates by geometric confinement, and thus promoting the emission of triplet excimer. Consequently, ultralong excimer RTP was finally achieved via tardily radiative transition from T_1* to S_0.

2.4 | Proof of universality and regulation of RTP properties

For the sake of verifying the generality of our approach and regulating the phosphorescence properties, we systematically investigated the impact of the chemical structure of Tpy derivatives on their RTP properties. A series of Tpy derivatives with different substituent groups on the 4,4′,4″ positions of Tpy core were rationally selected as shown in Figure 4 and Figure S1. It was found that the introduction of planar molecules such as Tpy-TriMe, Tpy-MeOH, Tpy-COOH, and Tpy-TriCOOH into the PVA matrix exhibited

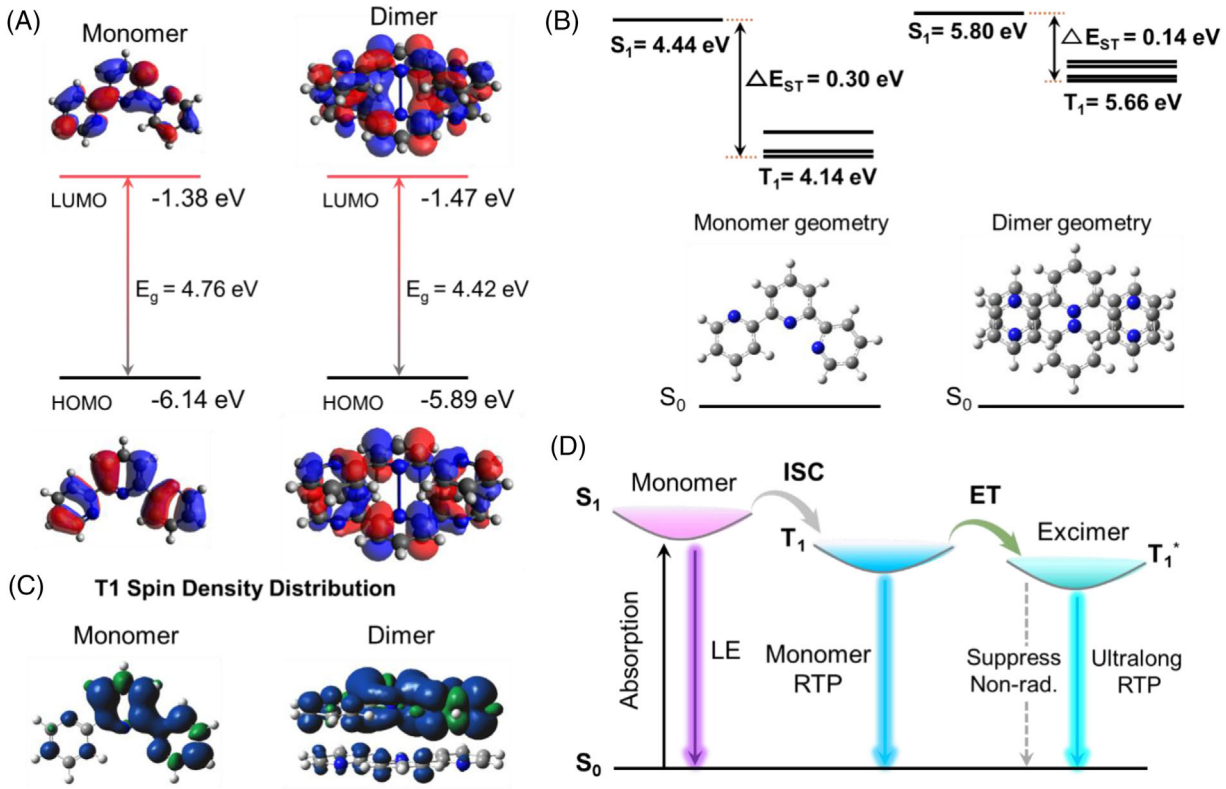

FIGURE 3 The density functional theory (DFT) calculation of PVA-Tpy system to prove ultralong excimer RTP. (A) Calculated frontier molecular orbitals and orbital energies, (B) vertical excitation energy levels, and (C) T_1 spin density distributions of monomeric and dimeric Tpy based on optimized ground-state geometry. (D) Simplified Jablonski diagram for interpreting ultralong excimer RTP.

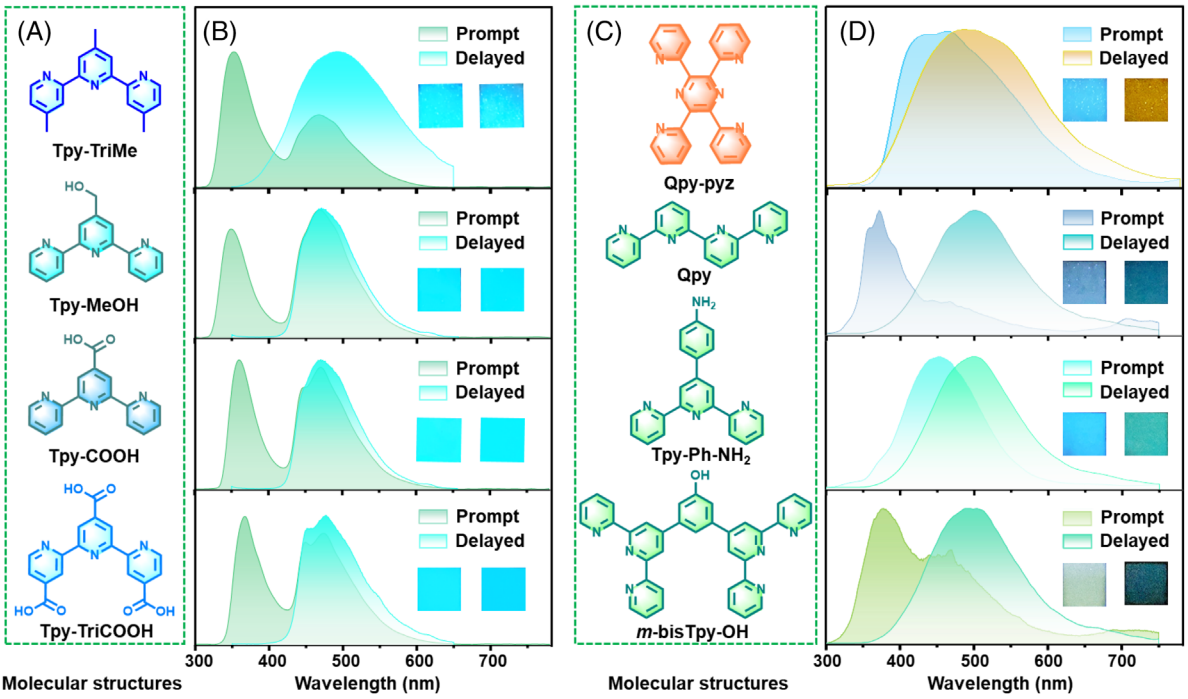

FIGURE 4 Molecular structures of Tpy derivatives and optical properties of RTP films doped with Tpy derivatives. (A) Molecular structures of Tpy derivatives (Tpy-TriMe, Tpy-MeOH, Tpy-COOH, Tpy-TriCOOH). (B) Prompt and delayed emission spectra of the Tpy derivatives-doped PVA films (delayed time: 0.05 ms), insets show the corresponding photos under 254-nm ultraviolet (UV) excitation (left) and after photo-excitation ceases (right). (C) Molecular structures of Tpy derivatives with larger conjugation (Qpy-pyz, Qpy, Tpy-Ph-NH_2, *m*-bisTpy-OH). (D) Prompt and delayed emission spectra of the Tpy derivatives-doped PVA films, insets show the corresponding photos under UV excitation (left) and after photo-excitation ceases (right), in the cases of PVA-(Tpy-Ph-NH_2) and PVA-(Qpy-pyz) films, 365 nm UV light was used.

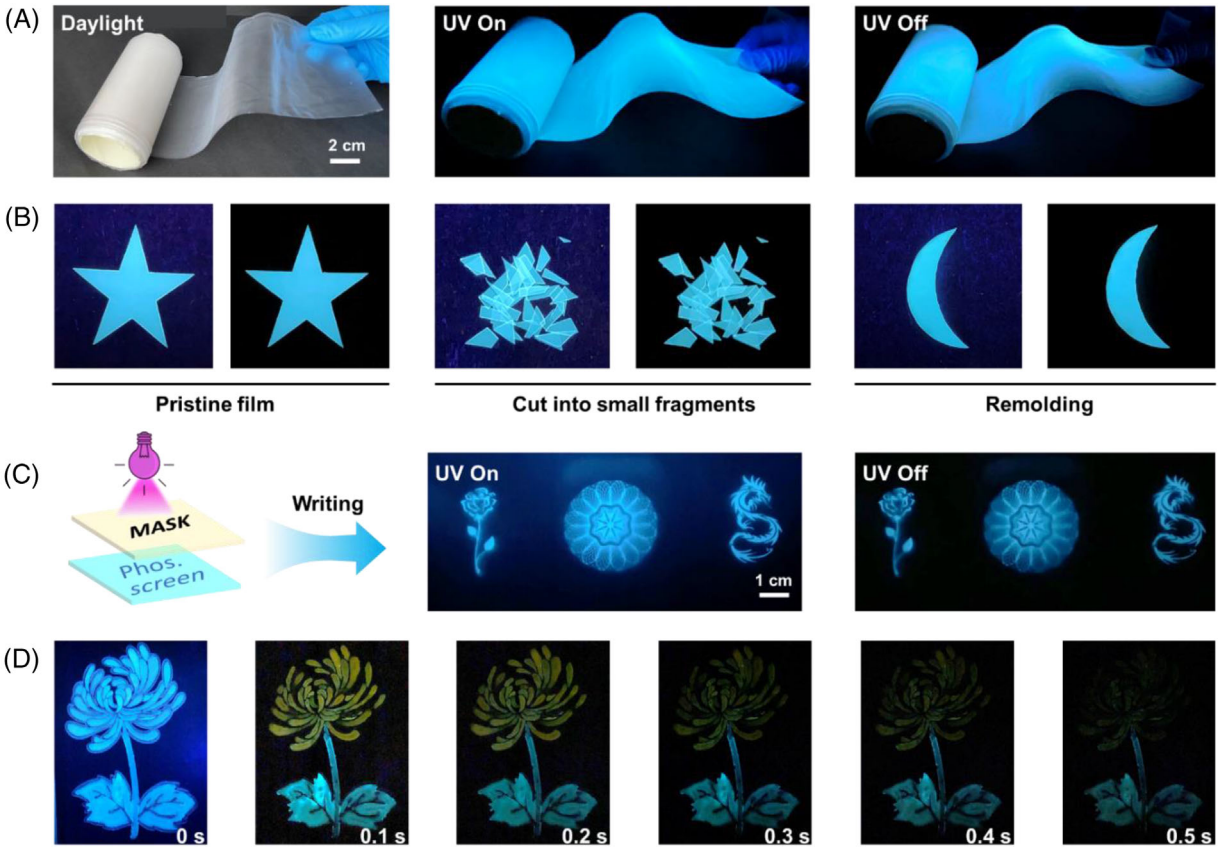

FIGURE 5 The large-area fabrication and applications of RTP films. (A) Photographs of a roll of flexible, transparent and large-scale PVA-Tpy film under daylight, 254-nm ultraviolet (UV) light and after erasing UV irradiation, respectively. (B) The processibility and remoldability of PVA-Tpy film, photographs were taken under 254-nm UV excitation (left) and after the removal of the UV irradiation (right). (C) The illustration of afterglow display by using large-area PVA-Tpy film as an imaging screen, photographs are corresponding patterns under 254 nm UV light and turning off UV light with photomasks. (D) The spatial-time-resolved encryption system by painting with PVA-(Tpy-Qpy-pyz) ("petals") and PVA-(Tpy-Ph-NH_2) ("leaves" and "rachis"), the photographs show the corresponding chrysanthemum pattern under 365-nm UV-on/off illuminations.

similar emission profile to those of PVA-Tpy film (Figure 4B and Figures S26–S27). Except for the PVA-(Tpy-TriMe), the RTP spectra and the fluorescent emission of excimer almost overlap. All films exhibited satisfying RTP performance with lifetime ranging from 331.3 to 379.3 ms (Figure S28). Importantly, the modification of Tpy skeleton with hydrogen-bonding donor or acceptor such as hydroxymethyl and carboxylic groups had a narrower phosphorescent emission band and lower ΔE_{ST} compared with Tpy (Table S3). On the contrary, a broader phosphorescence spectrum and larger ΔE_{ST} were observed for PVA-(Tpy-TriMe) film. No obvious afterglow was observed for PVA-Tpy-Tributyl and PVA-Tpy-Triester films (Figure S29) due to nonplanar structures of corresponding chromophores (Figure S1) leading to the lack of parallel alignment.[81] As such, we can conclude that the planar structure of organic phosphors is one of the key factors to obtain excellent RTP performance.

Encouraged by the above successful cases, we further extended the conjugation of chromophores to study its effect on afterglow properties. Tpy derivatives with larger conjugation including 2,3,5,6-tetra(pyridin-2-yl)pyrazine (Qpy-pyz), 2,2′;6′,2″;6″,2‴-quaterpyridine (Qpy), TPy-Ph-OH, Tpy-Ph-NH_2, *p*-bisTpy, and *m*-bisTpy-OH were designed and synthesized (Figure 4C and Figure S1). All compounds were fully characterized by ^1H and ^{13}C NMR (Figures S30–S39), and high-resolution electrospray ionization-time of Flight mass spectrometer. With the extension of aromatic conjugation, bluish-green afterglow was observed in the cases of PVA-(TPy-Ph-OH), PVA-(Tpy-Ph-NH_2), PVA-(*p*-bisTpy), PVA-(*m*-bisTpy-OH) RTP films (Figure 4D and Figure S40–S41). Impressively, golden afterglow with characteristic excimer emission was observed for PVA-(Qpy-pyz) film. In the case of PVA-(Tpy-Ph-NH_2) film, only excimer emission located at 452 nm was observed in the photoluminescence spectrum, which was consistent with excimer emission at the concentrated solution state (Figure S42). The delayed spectrum of PVA-(Tpy-Ph-NH_2) film exhibited a dominating emission at 498 nm with intense green afterglow. It further evidenced that the delayed emission of these RTP films originated from triplet excimer. Only dimly green afterglow was observerd for PVA-Qpy, PVA-(TPy-Ph-OH), PVA-(*p*-bisTpy), PVA-(*m*-bisTpy-OH) RTP films because of intense molecular vibrations. The lifetimes of these RTP films were in the order of tens of milliseconds (Figure S43). Additionally, we studied the RTP properties of films with phosphors containing single or double pyridine units as displayed in Figure S50. Compared with Tpy and its derivatives, the phosphorescence emission wavelength of these RTP films is still located in the range of 470-485 nm (Figure S50a–c), except for a shorter lifetime of tens of milliseconds (Figure S50d). These results manifested that the substituent groups and conjugation of Tpy derivatives play critical roles in the photophysical properties of RTP films including prompt and delayed emission, ΔE_{ST} and lifetime.

2.5 | Afterglow display and time-resolved information encryption

Generally, the self-standing and flexible RTP films with excellent performance are suitable for various applications including afterglow display, information encryption and anti-counterfeiting. By facilely doping Tpy derivatives into PVA matrix, aqueous precursor solution could be obtained in a large-scale. Subsequently, various transparent, flexible, and large-area RTP materials were successfully fabricated including films, fibers, coatings, patterns (Figure 5 and Figures S44–S48). As shown in Figure 5A and Video S3, a roll of transparent and flexible ultralong RTP film was successfully obtained by air drying and thermal annealing processes of the PVA-Tpy precursor solution on a preset template. The PVA-Tpy film demonstrated excellent thermal reprocessing for recycling based on the physical crosslinking of PVA chains (Figure 5B). By using this transparent and large-area film as an imaging screen, we were capable of realizing intelligent display as various fluorescent and afterglow patterns through the photomask method (Figure 5C). Taking advantage of the strong adhesion of PVA to various substrates such as paper, glass and cotton threads, we used the PVA-Tpy material as an afterglow paint and coating for anticounterfeiting (Figures S45–S48, Videos S4–7).

As a proof-of-concept, a spatial-time-dual-resolved encryption system was further developed on-demand.[82] The PVA-(Tpy-Ph-NH_2) and PVA-(Tpy-Qpy-pyz) were used as cryptographic paints to enable a chrysanthemum pattern (Figure 5D). Under the excitation of UV light, a cyan chrysanthemum pattern was visible to naked eye. In sharp contrast, a vivid chrysanthemum pattern with golden "petals", blue-green "leaves" and "stem" were observed immediately after the removal of UV light. The "petals" region faded into dark state, whereas "leaves" and "stem" regions remained blue-green afterglow at the delay time of 0.5 s. Benefiting from their excellent transparency, processability, and formability, these ultralong RTP materials have promising applications in the fields of information encryption and storage, intelligent display, anticounterfeiting.

3 | CONCLUSION

In summary, we have outlined a fundamental strategy to fabricate flexible, multicolor, and large-area excimer RTP with ultralong afterglow emission. Experimental results and theoretical calculations jointly unveil that the ultralong RTP originates from triplet excimer emission by synergistic effects of the self-assembly and geometric confinement. Tpy molecules were self-assembled and aggregated into uniform aggregates to enable the formation of excimer complexes, which is beneficial to promoting the ISC process by reducing ΔE_{ST}. The confinement by strong hydrogen-bonding interactions immensely restricts the motion of chromophores to inhibit energy dissipation. Adjusting the molecular structure of Tpy derivatives modulates the hydrogen-bonding interactions and aggregation, which leads to tunable RTP performance. Taking advantage of the excellent performance of these RTP materials, afterglow display, anticounterfeiting and time-resolved encryption systems were achieved on-demand. The current study not only points out the important role of aggregation and hydrogen bonding interactions in the generation of long-lived RTP but also provides fundamental insights into excimer phosphorescence.

ACKNOWLEDGMENTS

This project was financially supported by the National Key Research and Development Program of China (grant numbers: 2022YFB3204301 and 2021YFA1201201), the National Natural Science Foundation of China (grant numbers: 22205249 and U1967217), China Postdoctoral Science Foundation (grant numbers: 2021TQ0341 and 2022M723252), Zhejiang Provincial Natural Science Foundation of China (grant number: LQ23B040002), Natural Science Foundation of Ningbo (grant number: 2021J203), and Foundation of the Director of NIMTE (grant number: 2021SZKY0305).

CONFLICT OF INTEREST INTEREST

The authors declare no conflict of interests.

ORCID

Tao Chen https://orcid.org/0000-0001-9704-9545

REFERENCES

1. W. Zhao, Z. He, B. Z. Tang, *Nat. Rev. Mater.* **2020**, *5*, 869.
2. T. Maldiney, A. Lecointre, B. Viana, A. Bessière, M. Bessodes, D. Gourier, C. Richard, D. Scherman, *J. Am. Chem. Soc.* **2011**, *133*, 11810.
3. Y. Li, M. Gecevicius, J. Qiu, *Chem. Soc. Rev.* **2016**, *45*, 2090.
4. H.-J. Yu, Q. Zhou, X. Dai, F.-F. Shen, Y.-M. Zhang, X. Xu, Y. Liu, *J. Am. Chem. Soc.* **2021**, *143*, 13887.
5. R. Kabe, N. Notsuka, K. Yoshida, C. Adachi, *Adv. Mater.* **2016**, *28*, 655.
6. X.-Q. Liu, K. Zhang, J.-F. Gao, Y.-Z. Chen, C.-H. Tung, L.-Z. Wu, *Angew. Chem. Int. Ed.* **2020**, *59*, 23456.
7. F. Gu, X. Ma, *Chem. Eur. J.* **2022**, *28*, e202104131.
8. T. He, W.-J. Guo, Y.-Z. Chen, X.-F. Yang, C.-H. Tung, L.-Z. Wu, *Aggregate* **2023**, *4*, e250.
9. K. Leitonas, A. Tomkeviciene, G. Baratte, A. Dabuliene, S. M. Punniyakoti, D. Volyniuk, J. V. Grazulevicius, *Sens. Actuators B Chem.* **2021**, *345*, 130369.
10. E. Skuodis, K. Leitonas, A. Panchenko, L. Volyniuk, J. Simokaitienė, R. Keruckienė, D. Volyniuk, B. F. Minaev, J. V. Gražulevičius, *Sens. Actuators B Chem.* **2022**, *373*, 132727.
11. K. Jiang, Y. Wang, C. Cai, H. Lin, *Adv. Mater.* **2018**, *30*, 1800783.
12. J.-X. Wang, Y.-G. Fang, C.-X. Li, L.-Y. Niu, W.-H. Fang, G. Cui, Q.-Z. Yang, *Angew. Chem. Int. Ed.* **2020**, *59*, 10032.
13. J. Tan, Q. Li, S. Meng, Y. Li, J. Yang, Y. Ye, Z. Tang, S. Qu, X. Ren, *Adv. Mater.* **2021**, *33*, 2006781.
14. Y. Li, M. Gecevicius, J. Qiu, *Chem. Soc. Rev.* **2016**, *45*, 2090.
15. T. Zhang, X. Ma, H. Wu, L. Zhu, Y. Zhao, H. Tian, *Angew. Chem. Int. Ed.* **2020**, *59*, 11206.
16. Y. Zhang, Y. Su, H. Wu, Z. Wang, C. Wang, Y. Zheng, X. Zheng, L. Gao, Q. Zhou, Y. Yang, X. Chen, C. Yang, Y. Zhao, *J. Am. Chem. Soc.* **2021**, *143*, 13675.
17. X. Zhang, Y. Cheng, J. You, J. Zhang, C. Yin, J. Zhang, *Nat. Commun.* **2022**, *13*, 1117.
18. K. Jinnai, R. Kabe, Z. Lin, C. Adachi, *Nat. Mater.* **2022**, *21*, 338.
19. S. Kuila, S. J. George, *Angew. Chem. Int. Ed.* **2020**, *59*, 9393.
20. S. Cai, X. Yao, H. Ma, H. Shi, Z. An, *Aggregate* **2023**, https://doi.org/10.1002/agt2.320
21. H. Zhu, I. Badía-Domínguez, B. Shi, Q. Li, P. Wei, H. Xing, M. C. Ruiz Delgado, F. Huang, *J. Am. Chem. Soc.* **2021**, *143*, 2164.
22. W. Li, Q. Huang, Z. Mao, X. He, D. Ma, J. Zhao, J. W. Y. Lam, Y. Zhang, B. Z. Tang, Z. Chi, *Nat. Commun.* **2022**, *13*, 7423.
23. S. Garain, S. N. Ansari, A. A. Kongasseri, B. Chandra Garain, S. K. Pati, S. J. George, *Chem. Sci.* **2022**, *13*, 10011.
24. Z. An, C. Zheng, Y. Tao, R. Chen, H. Shi, T. Chen, Z. Wang, H. Li, R. Deng, X. Liu, W. Huang, *Nat. Mater.* **2015**, *14*, 685.

25. S. Cai, H. Shi, J. Li, L. Gu, Y. Ni, Z. Cheng, S. Wang, W. W. Xiong, L. Li, Z. An, W. Huang, *Adv. Mater.* **2017**, *29*, 1701244.
26. L. Gu, H. Wu, H. Ma, W. Ye, W. Jia, H. Wang, H. Chen, N. Zhang, D. Wang, C. Qian, Z. An, W. Huang, Y. Zhao, *Nat. Commun.* **2020**, *11*, 944.
27. X. Ma, C. Xu, J. Wang, H. Tian, *Angew. Chem. Int. Ed.* **2018**, *57*, 10854.
28. H. Peng, G. Xie, Y. Cao, L. Zhang, X. Yan, X. Zhang, S. Miao, Y. Tao, H. Li, C. Zheng, W. Huang, R. Chen, *Sci. Adv.* **2022**, *8*, eabk2925.
29. H. Gao, X. Ma, *Aggregate* **2021**, *2*, e38.
30. X. Ma, J. Wang, H. Tian, *Acc. Chem. Res.* **2019**, *52*, 738.
31. J. Han, W. Feng, D. Y. Muleta, C. N. Bridgmohan, Y. Dang, G. Xie, H. Zhang, X. Zhou, W. Li, L. Wang, D. Liu, Y. Dang, T. Wang, W. Hu, *Adv. Funct. Mater.* **2019**, *29*, 1902503.
32. Y. Wang, J. Yang, M. Fang, Y. Yu, B. Zou, L. Wang, Y. Tian, J. Cheng, B. Z. Tang, Z. Li, *Matter* **2020**, *3*, 449.
33. H. Sun, L. Zhu, *Aggregate* **2023**, *4*, e253.
34. X. Chen, C. Xu, T. Wang, C. Zhou, J. Du, Z. Wang, H. Xu, T. Xie, G. Bi, J. Jiang, X. Zhang, J. N. Demas, C. O. Trindle, Y. Luo, G. Zhang, *Angew. Chem. Int. Ed.* **2016**, *55*, 9872.
35. Z. Wang, C. Y. Zhu, J. T. Mo, X. Y. Xu, J. Ruan, M. Pan, C. Y. Su, *Angew. Chem. Int. Ed.* **2021**, *60*, 2526.
36. Y. Zhang, Y. Su, H. Wu, Z. Wang, C. Wang, Y. Zheng, X. Zheng, L. Gao, Q. Zhou, Y. Yang, X. Chen, C. Yang, Y. Zhao, *J. Am. Chem. Soc.* **2021**, *143*, 13675.
37. G. Jiang, J. Yu, J. Wang, B. Z. Tang, *Aggregate* **2022**, *3*, e285.
38. Q. Li, Z. Li, *Acc. Chem. Res.* **2020**, *53*, 962.
39. J. Yang, M. Fang, Z. Li, *Aggregate* **2020**, *1*, 6.
40. S. Cai, H. Shi, Z. Zhang, X. Wang, H. Ma, N. Gan, Q. Wu, Z. Cheng, K. Ling, M. Gu, C. Ma, L. Gu, Z. An, W. Huang, *Angew. Chem. Int. Ed.* **2018**, *57*, 4005.
41. E. Hamzehpoor, C. Ruchlin, Y. Tao, C.-H. Liu, H. M. Titi, D. F. Perepichka, *Nat. Chem.* **2023**, *15*, 83.
42. Y. Su, S. Z. F. Phua, Y. Li, X. Zhou, D. Jana, G. Liu, W. Q. Lim, W. K. Ong, C. Yang, Y. Zhao, *Sci. Adv.* **2018**, *4*, eaas9732.
43. L. Ma, S. Sun, B. Ding, X. Ma, H. Tian, *Adv. Funct. Mater.* **2021**, *31*, 2010659.
44. R. Tian, S. M. Xu, Q. Xu, C. Lu, *Sci. Adv.* **2020**, *6*, eaaz6107.
45. X. Yan, H. Peng, Y. Xiang, J. Wang, L. Yu, Y. Tao, H. Li, W. Huang, R. Chen, *Small* **2022**, *18*, 2104073.
46. C. K. Rhodes, *Excimer Lasers*, Springer: Berlin, Germany, **1984**.
47. A. P. de Silva, H. Q. N. Gunaratne, T. Gunnlaugsson, A. J. M. Huxley, C. P. McCoy, J. T. Rademacher, T. E. Rice, *Chem. Rev.* **1997**, *97*, 1515.
48. B. Ma, P. I. Djurovich, M. E. Thompson, *Coord. Chem. Rev.* **2005**, *249*, 1501.
49. M. Cocchi, J. Kalinowski, D. Virgili, J. A. G. Williams, *Appl. Phys. Lett.* **2008**, *92*, 113302.
50. M. Cocchi, J. Kalinowski, L. Murphy, J. A. G. Williams, V. J. O. E. Fattori, *Org. Electron.* **2010**, *11*, 388.
51. X. Wang, S.-L. Gong, D. Song, Z.-H. Lu, S. Wang, *Adv. Funct. Mater.* **2014**, *24*, 7257.
52. J. S. Kim, D. T. Quang, *Chem. Rev.* **2007**, *107*, 3780.
53. K. M. Chan, D. K. Kölmel, S. Wang, E. T. Kool, *Angew. Chem. Int. Ed.* **2017**, *56*, 6497.
54. Y. Zhang, H. Yang, H. Ma, G. Bian, Q. Zang, J. Sun, C. Zhang, Z. An, W.-Y. Wong, *Angew. Chem. Int. Ed.* **2019**, *58*, 8773.
55. R. M. Newcomb, J. S. Bangsund, K. W. Hershey, D. C. K. Rathwell, H.-Y. Na, J.-H. Jeon, P. Trefonas, R. J. J. A. P. L. Holmes, *Appl. Phys. Lett.* **2020**, *116*, 063302.
56. J. Ochi, K. Tanaka, Y. Chujo, *Angew. Chem. Int. Ed.* **2023**, *62*, e202214397.
57. X. Shan, W. Chi, H. Jiang, Z. Luo, C. Qian, H. Wu, Y. Zhao, *Angew. Chem. Int. Ed.* **2023**, *62*, e202215652.
58. R. Kabe, C. Adachi, *Nature* **2017**, *550*, 384.
59. K. Jinnai, R. Kabe, C. Adachi, *Adv. Mater.* **2018**, *30*, 1800365.
60. P. Alam, N. L. C. Leung, J. Liu, T. S. Cheung, X. Zhang, Z. He, R. T. K. Kwok, J. W. Y. Lam, H. H. Y. Sung, I. D. Williams, C. C. S. Chan, K. S. Wong, Q. Peng, B. Z. Tang, *Adv. Mater.* **2020**, *32*, 2001026.
61. J. Langelaar, R. P. H. Rettschnick, A. M. F. Lambooy, G. J. Hoytink, *Chem. Phys. Lett.* **1968**, *1*, 609.
62. E. A. Chandross, C. J. Dempster, *J. Am. Chem. Soc.* **1970**, *92*, 704.
63. N. J. Turro, M. Aikawa, *J. Am. Chem. Soc.* **1980**, *102*, 4866.
64. D. Yana, T. Shimizu, K. Hamasaki, H. Mihara, A. Ueno, *Macromol. Rapid Commun.* **2002**, *23*, 11.
65. R. D. Burkhart, N. I. Jhon, *J. Phys. Chem.* **1991**, *95*, 7189.
66. A. Cheng, Y. Jiang, H. Su, B. Zhang, J. Jiang, T. Wang, Y. Luo, G. Zhang, *Angew. Chem. Int. Ed.* **2022**, *61*, e202206366.
67. L. Liu, X. Wang, N. Wang, T. Peng, S. Wang, *Angew. Chem. Int. Ed.* **2017**, *56*, 9160.
68. D. Kim, J.-L. Brédas, *J. Am. Chem. Soc.* **2009**, *131*, 11371.
69. J.-X. Wang, L.-Y. Peng, Z.-F. Liu, X. Zhu, L.-Y. Niu, G. Cui, Q.-Z. Yang, *J. Phys. Chem. Lett.* **2022**, *13*, 1985.
70. Z. Liu, Y. Tian, J. Yang, A. Li, Y. Wang, J. Ren, M. Fang, B. Z. Tang, Z. Li, *Light Sci. Appl.* **2022**, *11*, 142.
71. S. K. Lower, M. A. El-Sayed, *Chem. Rev.* **1966**, *66*, 199.
72. C. Wang, L. Qu, X. Chen, Q. Zhou, Y. Yang, Y. Zheng, X. Zheng, L. Gao, J. Hao, L. Zhu, B. Pi, C. Yang, *Adv. Mater.* **2022**, *34*, 2204415.
73. T. Wang, A. K. Gupta, S. Wu, A. M. Z. Slawin, E. Zysman-Colman, *J. Am. Chem. Soc.* **2023**, *145*, 1945.
74. H. Du, W. Zhao, Y. Xia, S. Xie, Y. Tao, Y. Q. Gao, J. Zhang, X. Wan, *Aggregate* **2023**, *4*, e276.
75. F. M. Winnik, *Chem. Rev.* **1993**, *93*, 587.
76. S. Kuila, K. V. Rao, S. Garain, P. K. Samanta, S. Das, S. K. Pati, M. Eswaramoorthy, S. J. George, *Angew. Chem. Int. Ed.* **2018**, *57*, 17115.
77. S. Lohar, D. A. Safin, A. Sengupta, A. Chattopadhyay, J. S. Matalobos, M. G. Babashkina, K. Robeyns, M. P. Mitoraj, P. Kubisiak, Y. Garcia, D. Das, *Chem. Commun.* **2015**, *51*, 8536.
78. C. Lee, W. Yang, R. G. Parr, *Phys. Rev. B* **1988**, *37*, 785.
79. G. A. Petersson, T. G. Tensfeldt, J. A. Montgomery, *J. Chem. Phys.* **1991**, *94*, 6091.
80. H. Uoyama, K. Goushi, K. Shizu, H. Nomura, C. Adachi, *Nature* **2012**, *492*, 234.
81. Z. Wang, L. Gao, Y. Zheng, Y. Zhu, Y. Zhang, X. Zheng, C. Wang, Y. Li, Y. Zhao, C. Yang, *Angew. Chem. Int. Ed.* **2022**, *61*, e202203254.
82. H. Shi, S. Wu, M. Si, S. Wei, G. Lin, H. Liu, W. Xie, W. Lu, T. Chen, *Adv. Mater.* **2022**, *34*, 2107452.

SUPPORTING INFORMATION

Additional supporting information can be found online in the Supporting Information section at the end of this article.

How to cite this article: G. Yin, W. Lu, J. Huang, R. Li, D. Liu, L. Li, R. Zhou, G. Huo, T. Chen, *Aggregate* **2023**, *4,* e344. https://doi.org/10.1002/agt2.344